Oct4 redox sensitivity potentiates reprogramming and differentiation

Zuolian Shen,[1,2,6] Yifan Wu,[1,2,6] Asit Manna,[1,2] Chongil Yi,[2,3] Bradley R. Cairns,[2,3,4] Kimberley J. Evason,[1,2] Mahesh B. Chandrasekharan,[2,5] and Dean Tantin[1,2]

[1]Department of Pathology, University of Utah School of Medicine, Salt Lake City, Utah 84112, USA; [2]Huntsman Cancer Institute, University of Utah School of Medicine, Salt Lake City, Utah 84112, USA; [3]Department of Oncological Sciences, University of Utah School of Medicine, Salt Lake City, Utah 84112, USA; [4]Howard Hughes Medical Institute, University of Utah School of Medicine, Salt Lake City, Utah 84112, USA; [5]Department of Radiation Oncology, University of Utah School of Medicine, Salt Lake City, Utah 84112, USA

The transcription factor Oct4/Pou5f1 is a component of the regulatory circuitry governing pluripotency and is widely used to induce pluripotency from somatic cells. Here we used domain swapping and mutagenesis to study Oct4's reprogramming ability, identifying a redox-sensitive DNA binding domain, cysteine residue (Cys48), as a key determinant of reprogramming and differentiation. Oct4 Cys48 sensitizes the protein to oxidative inhibition of DNA binding activity and promotes oxidation-mediated protein ubiquitylation. *Pou5f1*^{C48S} point mutation has little effect on undifferentiated embryonic stem cells (ESCs) but upon retinoic acid (RA) treatment causes retention of Oct4 expression, deregulated gene expression, and aberrant differentiation. *Pou5f1*^{C48S} ESCs also form less differentiated teratomas and contribute poorly to adult somatic tissues. Finally, we describe *Pou5f1*^{C48S} (*Janky*) mice, which in the homozygous condition are severely developmentally restricted after E4.5. Rare animals bypassing this restriction appear normal at birth but are sterile. Collectively, these findings uncover a novel Oct4 redox mechanism involved in both entry into and exit from pluripotency.

[*Keywords*: Oct4 (Pou5f1); Oct1 (Pou2f1); induced pluripotent stem cells (iPSCs); oxidative stress; ubiquitylation]

Supplemental material is available for this article.

Received December 4, 2023; revised version accepted April 17, 2024.

The early mammalian embryo contains undifferentiated, pluripotent cells capable of generating all embryonic tissue lineages. Cultured embryonic stem cells (ESCs) have similar capabilities (Evans and Kaufman 1981). The transcription factor Oct4 governs the establishment of undifferentiated inner cell mass and epiblast cells, as well germline cells and ESCs (Schöler et al. 1990b; Morey et al. 2015). Both ESC differentiation and blastocyst implantation are followed by Oct4 loss (Nichols et al. 1998). Together with factors such as Nanog and Sox2, Oct4 forms a network of pluripotency regulators that enforce their own and each other's expression (Boyer et al. 2005).

Oct4 is widely used to generate induced pluripotent stem cells (iPSCs) from somatic cells (Takahashi and Yamanaka 2006). Reprogramming methods that omit Oct4 nevertheless rely on activation of the endogenous *Pou5f1* (*Oct4*) gene (Heng et al. 2010; Gao et al. 2013). Reprogramming strategies that increase efficiency (Esteban et al. 2010; Soufi et al. 2012; Vierbuchen and Wernig 2012; Costa et al. 2013; Rais et al. 2013) or improve the quality of iPSC clones (Yuan et al. 2011; Buganim et al. 2014; Chen et al. 2015; Velychko et al. 2019) reveal trade-offs: efficiently generating iPSCs that are of nonoptimal quality or inefficiently generating iPSCs with improved developmental potential.

Pluripotent cells coexpress Oct4 together with the widely expressed prototypic POU transcription factor Oct1/Pou2f1 (Okamoto et al. 1990; Rosner et al. 1990; Suzuki et al. 1990). The two proteins share similar DNA binding domains (DBDs) and consensus DNA binding sequences (Tantin 2013). They also associate with many of the same target genes (Ferraris et al. 2011; Perovanovic et al. 2023). Nevertheless, Oct1 and other mammalian Oct4 paralogs do not efficiently reprogram (Takahashi and Yamanaka 2006; Feng et al. 2009). In contrast, other reprogramming factors such as Sox2, Klf4, and c-Myc can be replaced with close paralogs (Nakagawa et al. 2008; Shi et al. 2008). Structure/function studies comparing Oct4 with its paralogs have identified reprogramming

[6]**These authors contributed equally to this work.**
Corresponding author: dean.tantin@path.utah.edu
Article published online ahead of print. Article and publication date are online at http://www.genesdev.org/cgi/doi/10.1101/gad.351411.123.

determinants (Esch et al. 2013; Jin et al. 2016; Jerabek et al. 2017). An example is three amino acid residues that are in the Oct4 DBD but absent in Oct6/Pou3f1 that are needed to form Sox2 heterodimers. Introducing these residues, plus the Oct4 N and C termini, into Oct6 results in efficient reprogramming (Jerabek et al. 2017). Interestingly, several Oct4 paralogs, including Oct1, contain these residues but are still reprogramming-incompetent, indicating the presence of additional reprogramming determinants in Oct4 (and Oct6) that are absent in Oct1.

Recent studies show that omission of Oct4 from reprogramming cocktails, despite being inefficient, results in qualitatively superior iPSC clones with enhanced developmental potential (An et al. 2019; Velychko et al. 2019). The counterproductive activities of Oct4 are caused by transient promotion of gene expression programs that deviate cells from correct reprogramming trajectories (Velychko et al. 2019). A logical extension of these findings is that transient mitigation of counterproductive Oct4 activities may enable reprogramming.

Here, we identify an Oct4 DBD cysteine residue (Cys48) as a central reprogramming determinant. A serine residue is present in Oct1 at this position. In the presence of the Oct4 N terminus, mutating Oct1's serine to cysteine confers robust reprogramming activity. Conversely, mutating Oct4's cysteine to serine reduces reprogramming efficiency by ~60%. Cys48 sensitizes Oct4 DNA binding activity to oxidative stress and potentiates protein ubiquitylation. CRISPR-edited Oct4^{C48S} embryonic stem cell (ESC) lines are phenotypically normal until differentiated, after which they abnormally retain Oct4 protein expression and pluripotency gene expression signatures. Differentiating Oct4^{C48S} cells proliferate less and undergo apoptosis at higher rates compared with parental controls. Mutant ESCs also form less differentiated teratomas and contribute poorly to the development of viable adult mice. Oct4^{C48S} mutant mice (dubbed *Janky* mice [*Jky*]) appear phenotypically normal and fertile in the heterozygous condition, whereas homozygotes are severely developmentally restricted after the blastocyst stage. Cumulatively, our findings identify an Oct4 redox sensitivity mechanism that restrains protein function but nevertheless functions positively in reprogramming and normal differentiation.

Results

Oct4 vs. Oct1 reprogramming potential concentrates in a DBD cysteine

The two DNA binding subdomains of mouse Oct1 and Oct4, termed the POU-specific domain (POU_S) and POU homeodomain (POU_H), share 71% and 59% identity, respectively (Fig. 1A). In contrast, the N and C termini and the linker between the subdomains are divergent. The human proteins are structured similarly. The high similarity allows the amino acid numbering of the DBDs to be standardized by referring to the first amino acid of POU_S as residue 1 (Fig. 1A). To measure reprogramming efficiency, we transduced mouse embryonic fibroblasts (MEFs) expressing GFP under the control of endogenous *Pou5f1* (Lengner et al. 2007) with lentiviruses expressing the four Yamanaka factors (Fig. 1B; Sommer et al. 2009). To identify Oct4 determinants important for reprogramming, we replaced Oct4 within this construct with Oct1 or chimeric proteins containing the distinct DBDs and N and C termini (Fig. 1B). We included C-terminal FLAG tags on all proteins to track expression. Unlike an N-terminal FLAG tag, which was deleterious to Oct4 (Supplemental Fig. S1), a C-terminal FLAG tag reprograms with similar efficiency (Fig. 1C). Prior work comparing Oct4 with Oct6 identified Oct4 K40 (Fig. 1A) as important for reprogramming (Jin et al. 2016). We therefore also mutated Oct1^{N40} within POU_S to lysine in some constructs (N40K) (Fig. 1B). Substituting Oct1 for Oct4 eliminated reprogramming potential (Fig. 1D,E), setting a baseline for domain swaps and mutations. All of the chimeric constructs showed poor activity, with constructs containing the Oct4 N terminus generating the most colonies (~5% the level of WT Oct4) (Fig. 1D,E). These findings are consistent with work establishing the importance of the Oct4 N terminus (Boija et al. 2018). Similar data were obtained at multiple time points (Supplemental Fig. S2A), indicating that the results reflect qualitative rather than kinetic differences. Anti-FLAG immunoblotting showed similar expression (Fig. 1F). Viral titers from six tested vectors from this experiment were also similar (Supplemental Fig. S2B). Because a construct with both the Oct4 N and C termini ("4N/C") displayed only ~5% efficiency (Fig. 1D,E), we conclude that determinants within the Oct4 DBD confer the bulk of reprogramming potential vis-à-vis Oct1.

In the context of the Oct4 N terminus ("4N"), we mutagenized DBD amino acid residues that differ between Oct1 and Oct4, focusing on post-translationally modifiable residues: Lys, Ser, Thr, and Cys. This analysis identified 14 different amino acids, not including Lys40 (Fig. 1A). Oct6 is capable of reprogramming when modified to enable Sox2 dimerization (Kim et al. 2020). Filtering these residues using conservation between Oct4 and Oct6 pinpointed six possible residues. Replacing one of these, Oct1 Ser48, with the Oct4 cysteine residue found at this position increased activity more than sevenfold over the "4N" construct containing the Oct4 N terminus alone (Fig. 2A,B, 1–4All). iPSC colonies formed under these conditions showed a pluripotent morphology and expressed GFP from the endogenous *Pou5f1* locus at levels comparable with Oct4 (Supplemental Fig. S3). The remaining activity was concentrated in the linker domain, as a construct containing the Oct4 N terminus, Cys48, and the Oct4 linker (4N/L-S48C) had 100% activity (Fig. 2A,B). The Oct4 linker has been shown to regulate reprogramming via selective interactions with different cofactors (Esch et al. 2013; Han et al. 2022). The differences were maintained over time, with the 1–4All construct consistently generating ~60% activity over multiple days, indicating that the differences were not kinetic in nature (Supplemental Fig. S4A). Similar results were obtained using normal primary MEFs and assessing alkaline phosphatase-positive rather than GFP-positive iPSCs (Supplemental Fig. S4B,C).

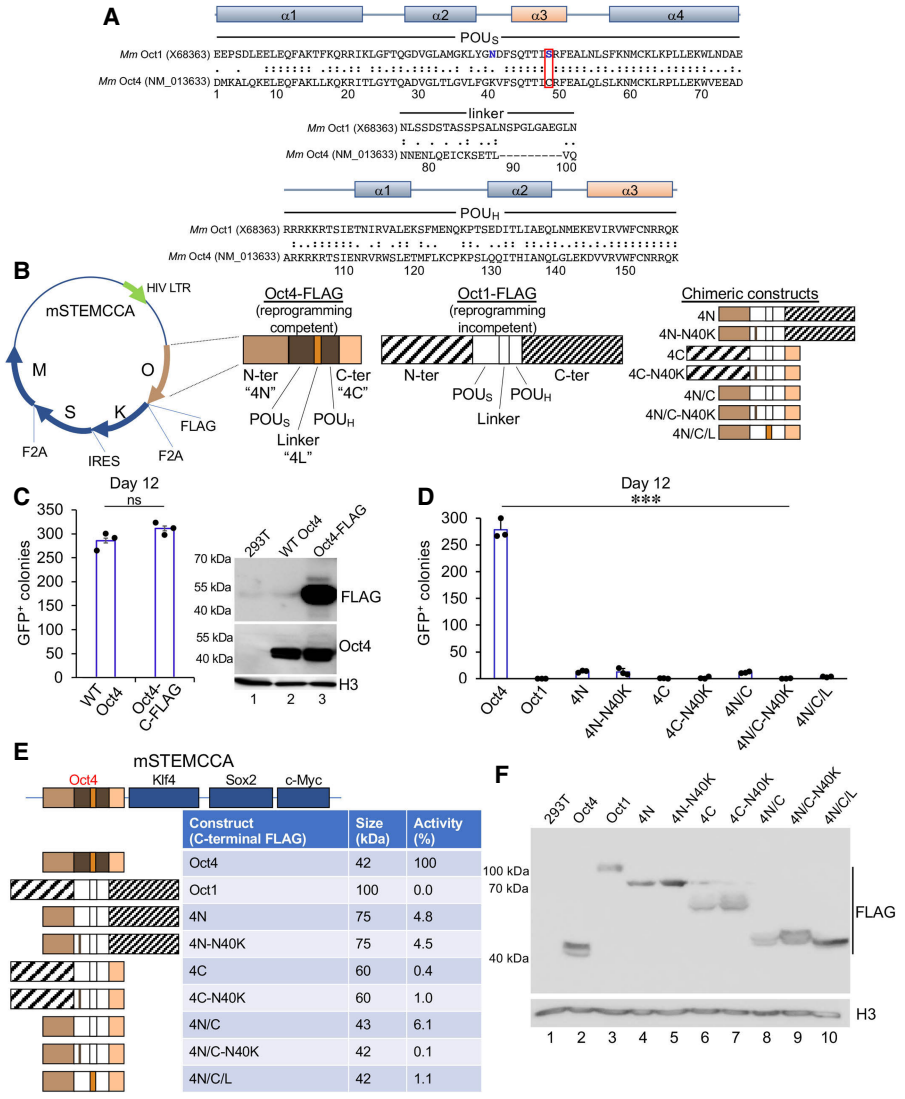

Figure 1. Oct4 reprogramming activity vis-à-vis Oct1 maps to the DBD. (*A*) Mouse Oct1 versus Oct4 DBD alignment. POU_S and POU_H refer to the two DNA binding subdomains. Asparagine 40 (blue) was mutated to lysine in some constructs. The key Oct1 serine 48 residue (cysteine in Oct4) is boxed in red. (*B*) Schematic of the reprogramming vector with C-terminal Oct4 FLAG tag. (HIV) Human immunodeficiency virus, (LTR) long terminal repeat, (O) Oct4, (K) Klf4, (S) Sox2, (M) c-Myc. The different domains of Oct4 and Oct1 are color-coded. Chimeric constructs are shown at the *right*. The construct name indicates which domain of Oct4 is included, separated by slashes; e.g., 4N/C indicates the Oct4 N and C termini fused to the rest of Oct1. Point mutations are shown with a dash. (*C*) Reprogramming activity of C-terminally tagged Oct4 relative to the untagged control. Results show an average of $N = 3$ independent experiments. Anti-FLAG and anti-Oct4 immunoblots using tagged and untagged constructs transiently transfected into 293T cells are shown at the *right*. (*D*) iPSC formation assay using target Oct4-GFP MEFs. Reprogramming was assessed using the number of GFP-expressing iPSC colonies. Oct4 was used as a positive control, and Oct1 was used as a negative control. All constructs bore C-terminal FLAG tags. $N = 3$ experiments were performed. (*E*) Schematic and summary of size and activity of the constructs used in *D*. To determine the percentage of activity, the averaged colony count using Oct4 in *D* was set to 100%. For simplicity, C-terminal FLAG tags are not shown. (*F*) Anti-FLAG immunoblot showing expression of the different constructs when transiently transfected into 293T cells transduced with the reprogramming vectors. Histone H3 is shown as a loading control.

An $Oct4^{C48S}$ construct reduced activity by 60% (Fig. 2A,B), indicating that over half of Oct4's differential reprogramming activity vis-à-vis Oct1 operates through this residue. The reciprocal $Oct1^{S48C}$ mutation did not reprogram (Fig. 2A,B, Oct1-S48C), indicating that Cys48 is not sufficient and highlighting its combined importance with the Oct4 N terminus for reprogramming. The proteins were equivalently expressed (Fig. 2C). These results indicate that in the context of the Oct4 N terminus, Cys48 confers robust reprogramming activity. In an Oct1 DBD:DNA structure (Klemm et al. 1994), Ser48 hydrogen bonds with the DNA backbone (Fig. 2D). In an Oct4:Sox2:nucleosome structure (Michael et al. 2020), the Cys48 sulfhydryl also allows for hydrogen bonding.

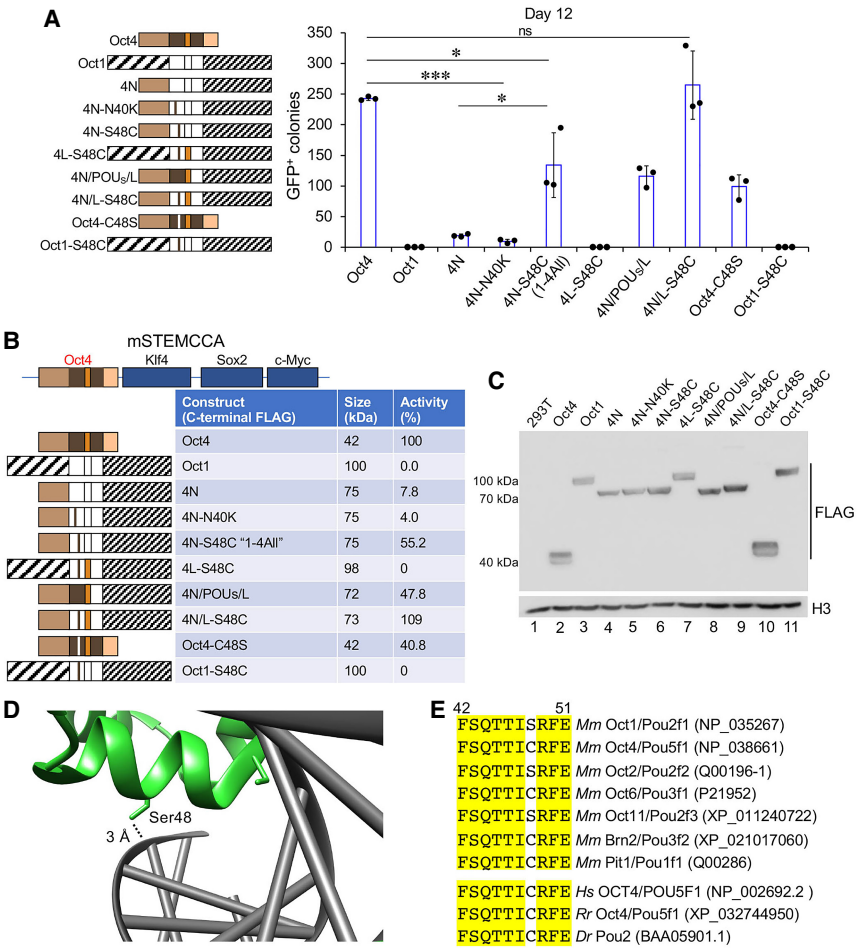

Construct (C-terminal FLAG)	Size (kDa)	Activity (%)
Oct4	42	100
Oct1	100	0.0
4N	75	7.8
4N-N40K	75	4.0
4N-S48C "1-4All"	75	55.2
4L-S48C	98	0
4N/POUs/L	72	47.8
4N/L-S48C	73	109
Oct4-C48S	42	40.8
Oct1-S48C	100	0

Figure 2. Activity of Oct4 cysteine 48 in reprogramming. (*A*) iPSC formation assay using Oct1–Oct4 lentiviral constructs that manipulate cysteine 4. Oct4 was used as a positive control, and Oct1 was used as a negative control. All constructs bore C-terminal FLAG tags. $N = 3$ experiments. (*B*) Schematic and summary of size and activity of the constructs used in *A*. The activity of Oct4 in *A* was set to 100%. (*C*) Anti-FLAG immunoblot showing expression of the different constructs when transiently transfected into 293T cells transduced with the reprogramming vectors. Histone H3 is shown as a loading control. (*D*) Detail from an Oct1:octamer DNA cocrystal structure (PDB ID: 1OCT) (Klemm et al. 1994) showing Ser48 making hydrogen bond contacts with the DNA backbone. (*E*) Paralog comparison of mouse POU protein amino acid residues corresponding to α-helix 3 of the POU_S subdomain.

Predictably, Cys48 mutation to glycine greatly diminishes Oct4 DNA binding in vitro (Marsboom et al. 2016). Oct6 also contains a cysteine at this position, as does human Oct4 (Fig. 2E). The *Danio rerio* Oct1/4 paralog Pou2 also contains a cysteine at this position (Fig. 2E), suggesting that cysteine may be the ancestral residue. These structural studies and our findings indicate that Ser48 and Cys48 have minimal differences in DNA binding but that Cys48 nevertheless plays key roles in reprogramming.

Oct4 Cys48 mediates degradation in response to oxidative stress

Oct4 is hypersensitive to oxidative stress (Lickteig et al. 1996; Guo et al. 2004; Marsboom et al. 2016) in a manner reversed by thioredoxin (Guo et al. 2004), implicating cysteine thiols in redox sensitivity. We reproduced this result using electrophoretic mobility shift assays (EMSAs) and DNA containing a canonical binding element (Supplemental Fig. S5), suggesting that Cys48 may potentiate reprogramming through a redox mechanism. We used lysates from 293T cells transfected with WT or C48S Oct4 to measure DNA binding. To measure redox sensitivity, we pretreated Oct4 with the oxidizing agent diamide prior to addition of DNA. 293T cells express endogenous Oct1 as an internal control (Fig. 3A, lanes 2,3). Oct4 bound to octamer DNA specifically (Fig. 3A, lanes 7,8) and was hypersensitive to diamide treatment (Fig. 3A, lanes 9–11). $Oct4^{C48S}$ bound DNA equivalently (Fig. 3A, lane 13) but was comparatively resistant to oxidation (Fig. 3A, lanes 14–16). In contrast, little sensitivity was observed with Oct1. Quantification from three replicates is shown in Figure 3B. The recombinant Oct4 contained a C-terminal FLAG tag, allowing for purification (Supplemental Fig. S6). Similar relative resistance to oxidative inhibition of DNA binding was observed using purified recombinant C48S Oct4 (Fig. 3C). Quantification from three replicates is shown in Figure 3D. These results indicate that Oct4 Cys48 mediates oxidative inhibition of DNA binding.

Oct4 oxidation has been linked to its degradation (Marsboom et al. 2016). We noted in overexposed immunoblots the presence of multiple slow-migrating high-molecular-weight forms of wild-type Oct4 that were attenuated with C48S mutation (Fig. 3E, lanes 2,3). Hydrogen peroxide treatment augmented the banding pattern using wild-type but not mutant protein (Fig. 3E, lanes 4,5). The bands were also increased using MG-132, consistent with ubiquitylated species (Fig. 3E, lanes 6,7). H_2O_2 and MG-132

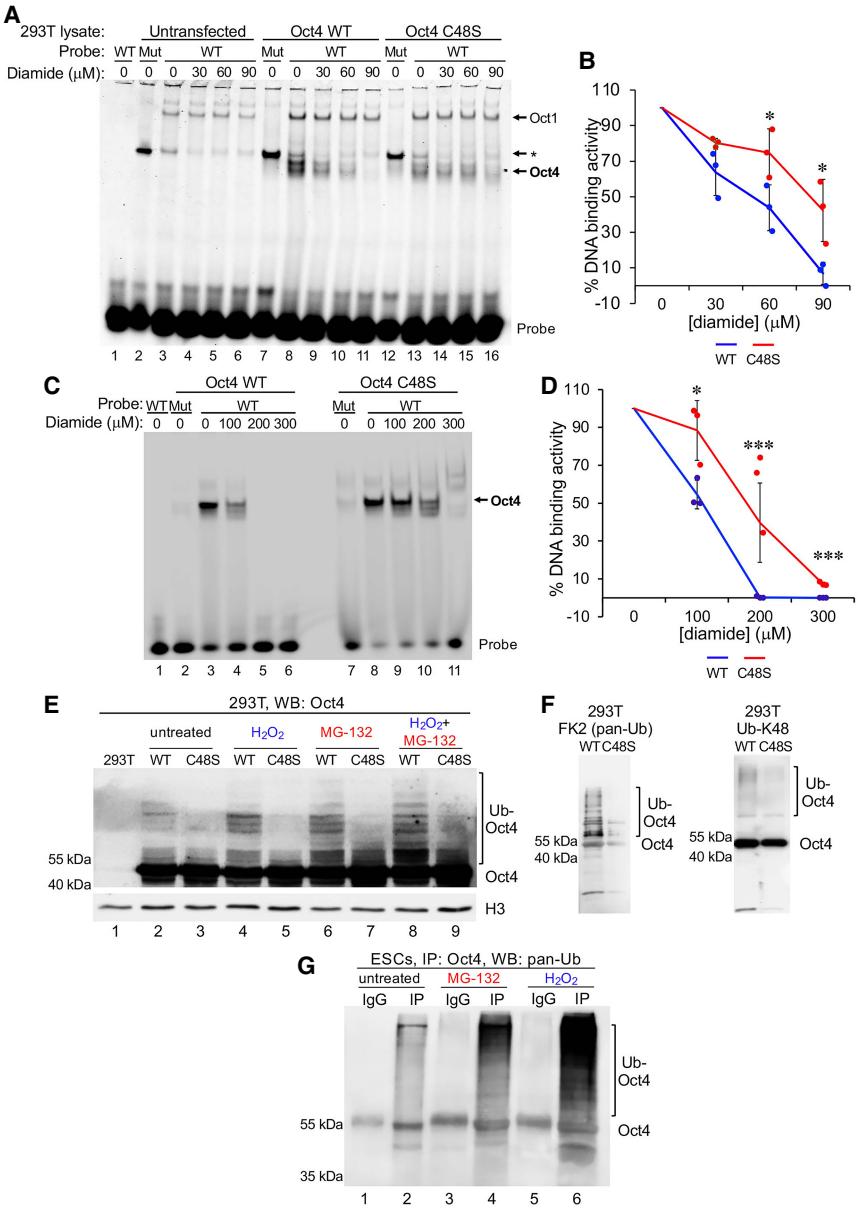

Figure 3. Oct4 cysteine 48 confers DNA sensitivity to oxidative stress and oxidative stress-induced ubiquitylation. (*A*) EMSAs using canonical octamer DNA and wild type of C48S full-length Oct4. 293T cells were transiently transfected with plasmids encoding C-terminal FLAG-tagged Oct4 constructs. Protein lysates were made and immediately used for EMSAs with increasing amounts of diamide. The larger redox-resistant Oct1 protein that binds the wild-type (WT) but not the mutant (Mut) probe is highlighted with an arrow. An asterisk indicates a redox-sensitive band with superior binding to mutant rather than octamer DNA. (*B*) Quantification of Oct4 band intensity relative to no diamide, which was set to 100%. $N=3$ independent experiments. (*C*) Oct4 containing a C-terminal streptavidin tag was purified from 293T cell lysates using anti-FLAG beads. Isolated protein was used in assays similar to in *A*. (*D*) Quantification of *C* and two similar experiments. (*E*) Highly exposed Oct4 immunoblot using lysates prepared from 293T cells transfected with constructs expressing C-terminally FLAG-/twin-strep-tagged Oct4. Subsets of cells were pretreated with 1 mM H_2O_2 for 2 h, 10 μM MG-132 for 2 h, or both. All samples contained MG-132 in the lysis buffer to prevent degradation. Histone H3 is shown as a loading control. (*F*) Purified wild-type and C48S Oct4 was immunoblotted using antibodies against specific ubiquitin linkages. (*G*) Oct4 and control immunoprecipitates from wild-type ESCs were immunoblotted using FK2 antibodies. Cells were treated with 10 μM MG-132 for 2 h or 2.5 mM H_2O_2 for 2 h.

cotreatment further increased the pattern (Fig. 3E, lanes 8,9). None of these treatments affected short-term cell viability (Supplemental Fig. S7).

We immunoblotted purified Oct4 with antibodies specific to different ubiquitin species. Antibodies recognizing both monoubiquitylated and polyubiquitylated proteins revealed strong diminution with $Oct4^{C48S}$, as expected (Fig. 3F, FK2). Diminution was observed with K48 linkage-specific polyubiquitin antibodies (Fig. 3F), whereas K63 linkage-specific antibodies showed modest differences (Supplemental Fig. S8). Similar ubiquitylated species were observed using endogenous Oct4 in wild-type ESCs (Fig. 3G, lane 2) that were augmented by H_2O_2 and MG-132 (Fig. 3G, lanes 4,6). We conclude that Cys48 promotes Oct4 ubiquitylation and degradation in response to oxidative stress, at least in part via catalysis of K48-linked polyubiquitin chains.

$Oct4^{C48S}$ ESCs differentiate abnormally

We generated ESCs with a single-base missense mutation in the endogenous *Oct4* (*Pou5f1*) locus that converts Cys48 to Ser. Two silent point mutations were also engineered to create an XbaI site to monitor targeting and facilitate genotyping. Three low-passage parent ESC lines of different strain backgrounds were chosen for targeting. Multiple independent clones were generated for each line. Homozygous mutation was confirmed by high-resolution melting analysis and resequencing (Fig. 4A; Supplemental Fig. S9A). Tested clones were karyotypically normal and similar to parent ESCs, with the proportion of diploid cells ranging between 71% and 93%. Undifferentiated mutant ESC clones expressed Oct4, Sox2, and Nanog at similar levels and were morphologically indistinguishable from their parent clones (Fig. 4B–D; Supplemental Fig. S9B–D).

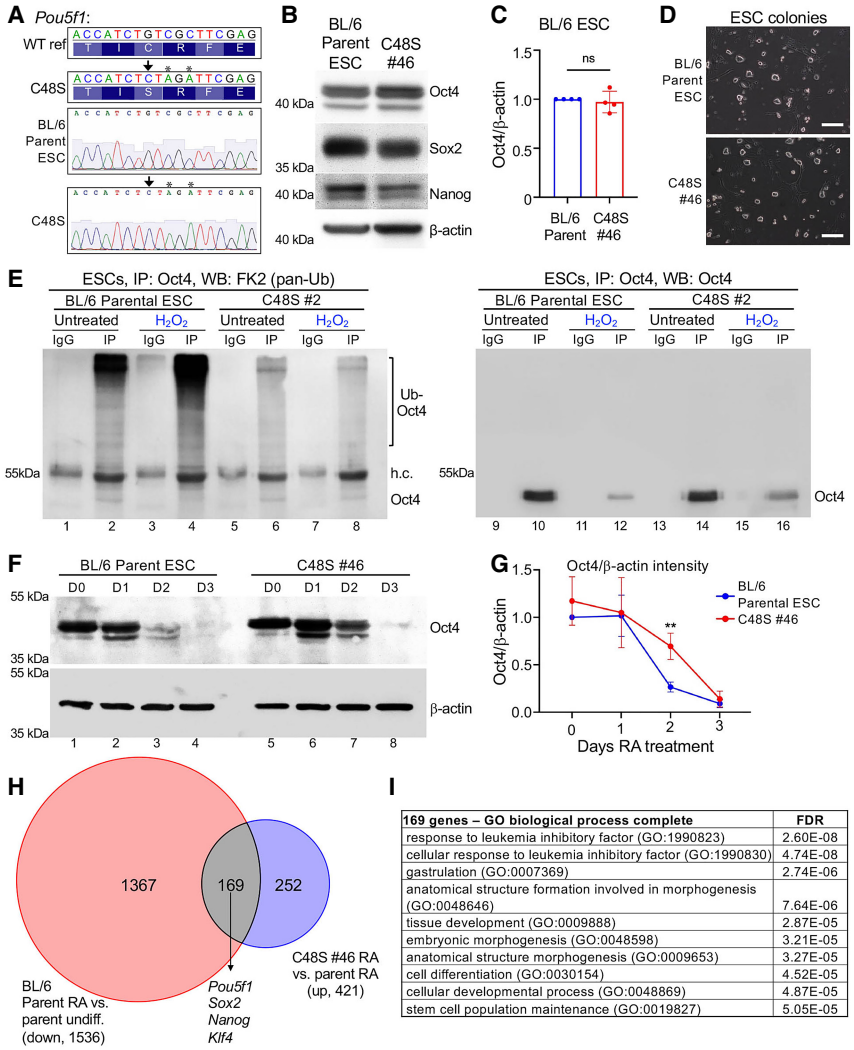

169 genes – GO biological process complete	FDR
response to leukemia inhibitory factor (GO:1990823)	2.60E-08
cellular response to leukemia inhibitory factor (GO:1990830)	4.74E-08
gastrulation (GO:0007369)	2.74E-06
anatomical structure formation involved in morphogenesis (GO:0048646)	7.64E-06
tissue development (GO:0009888)	2.87E-05
embryonic morphogenesis (GO:0048598)	3.21E-05
anatomical structure morphogenesis (GO:0009653)	3.27E-05
cell differentiation (GO:0030154)	4.52E-05
cellular developmental process (GO:0048869)	4.87E-05
stem cell population maintenance (GO:0019827)	5.05E-05

Figure 4. Oct4^{C48S} ESCs are phenotypically normal but retain Oct4 expression when differentiated. (*A*, *top*) Schematic for CRISPR-mediated *Pou5f1* (*Oct4*) mutation. A single nucleotide change (arrow) converts the wild-type cysteine to the serine present in Oct1. Asterisks indicate two silent point mutations present in the guide RNA to monitor mutagenesis. (*Bottom*) DNA sequencing trace of a homozygous mutant clone. (*B*) An example C57BL/6 ESC clone (#46) was immunoblotted for Oct4, Sox2, and Nanog, and β-actin was used as a loading control. (*C*) Quantification of Oct4 protein levels from $N = 4$ immunoblots. Levels were normalized to β-actin. (*D*) Example images of pluripotent colonies from a parental ESC line and a derived Oct4^{C48S} ESC line (#46). Images were collected at 10× magnification. Scale bar, 0.2 mm. (*E*) Pan-Ub and control Oct4 immunoblots of Oct4 immunoprecipitates from parent and Oct4^{C48S} (clone #2) ESC lines. Cells were grown on gelatin without feeders. Normal culture medium was replaced with medium lacking supplemental glutamine and β-mercaptoethanol 2 h prior to the experiment. Where indicated, cells were treated with 2.5 mM H_2O_2 for a further 2 h. Oct4 was immunoprecipitated using a rabbit polyclonal antibody (Abcam) and immunoblotted using monoclonal mouse antibodies against pan-Ub and Oct4. (*F*) Parent or derived Oct4^{C48S} ESCs were differentiated using RA. Lysates were collected at the indicated times and probed for Oct4 by immunoblotting. β-Actin was used as a loading control. (*G*) Average quantified Oct4/β-actin levels from $N = 3$ immunoblots conducted with mutant ESC clone #46. (*H*) mRNA from parental and #46 mutant cells differentiated for 2 days with RA and undifferentiated controls were transcriptionally profiled using RNA-seq. Significantly increased genes in differentiating C48S relative to parent cells (421 genes) were intersected with the set of genes downregulated in parental cells upon differentiation (1536 genes) to yield 169 genes. (*I*) PANTHER GO terms associated with 169 genes from *G* identified using the "biological process" ontology.

To test whether C48S mutation protects endogenous Oct4 against oxidative stress, we studied Oct4 ubiquitination in parent and mutant ESCs. Oct4 was immunoprecipitated from ESC lysates, and the resulting material was immunoblotted using pan-Ub (FK2) and Oct4 antibodies. Ubiquitylation of endogenous Oct4 in ESCs was clearly visualized and increased with H_2O_2 exposure (Fig. 4E, lanes 1–4), whereas Oct4^{C48S} ubiquitylation was attenuated (Fig. 4E, lanes 5,6) and unaffected by oxidative stress (Fig. 4E, lanes 7,8). Oct4 immunoblotting confirmed that the protein was immunoprecipitated, with decreased Oct4 recovered with oxidative stress in parental cells, and more Oct4 recovered in mutant cells (Fig. 4E, right panel).

Cells were then differentiated in vitro using retinoic acid (RA) to assess Oct4 expression, morphology, and cell counts. Oct4 protein expression was abnormally retained early during differentiation (Fig. 4F, lanes 3,7). Quantification from multiple experiments revealed that the effect was transient, with a >2.8-fold increase of Oct4 at day 2 that normalized by day 3 (Fig. 4G). Similar results were obtained using the same clone compared with parent cells electroporated without CRISPR ribonucleoprotein (RNP) (Supplemental Fig. S9E). These results were recapitulated using a second clone from the same parental ESC line (Supplemental Fig. S9F), as well as a clone from a different 129×C57BL/6 ESC line, which differentiated more slowly and showed greater differences (Supplemental Fig. S9G).

We performed transcriptional profiling of parent and mutant cells at RA differentiation day 2, as well as undifferentiated controls. Three replicates per condition were used, which showed tight concordance (Supplemental Fig. S10A). Twenty million to 31 million sequence reads were generated for each sample, ~80% of which aligned to the *mm39* reference genome. We identified 421 genes

with significantly elevated gene expression in differentiating mutant relative to parent cells ($P < 0.001$, >2.5-fold) (Fig. 4H; Supplemental Table S1). Intersecting these genes with the set of genes normally decreased upon differentiation of parent cells at this time point (1536 genes) showed that 40% of the 421 genes with retained expression in mutant cells (169 genes) are normally downregulated with differentiation. These included *Oct4* itself (*Pou5f1*), as well as *Sox2*, *Nanog*, and *Klf4* (Fig. 4H). Comparing these genes with established Oct4 ChIP-seq (King and Klose 2017) identified 114 of 169 genes (67%) as direct Oct4 targets (Supplemental Table S1). The complete set of 169 genes was enriched for gene ontology (GO) terms associated with pluripotency such as "response to leukemia inhibitory factor" (including *Pou5f1*, *Klf4*, and *Fgf4*) and "stem cell population maintenance" (including *Nanog*, *Pou5f1*, *Sox2*, and *Fgf4*) (Fig. 4I). Similar results were obtained using a hierarchical clustering approach. We used the 100 most differentially expressed genes upon differentiation for both genotypes (150 total genes). Although the differentiating parental and mutant replicates clustered together, there was a cohort of pluripotency-associated genes (including *Pou5f1*) whose downregulation was blunted in mutant cells (Supplemental Fig. S10B). A second cohort of differentiation-specific genes showed poorer expression in mutant cells upon differentiation. These included *Krt18*, *Mest*/*Peg1*, and *Dag1* (Supplemental Fig. S10B). Comparing the complete set of 150 genes with Oct4 ChIP-seq (King and Klose 2017) identified 117 (78%) as direct Oct4 targets (Supplemental Table S1). These results indicate that Oct4^{C48S} ESCs inappropriately delay loss of pluripotency gene expression signatures during differentiation.

The level and duration of retained Oct4 expression during differentiation can affect lineage specification (Wang et al. 2012; Aksoy et al. 2013; DeVeale et al. 2013; Radzisheuskaya et al. 2013). To determine the effects of Oct4^{C48S} mutation on differentiation, we visualized cells treated with RA microscopically. These experiments revealed a significant depletion of cells beginning at RA differentiation day 3 (Fig. 5A,B, D6–D12). The decreased cell numbers could be due to decreased proliferation and/or increased cell death. We studied proliferation using cell trace violet (CTV) and apoptosis using TUNEL staining. Adherent, viable differentiating C48S cells showed decreased proliferation at days 3 and 4 (Fig. 5C) and increased apoptosis at day 2 (Fig. 5D). ESCs differentiating with RA also experience an increase in global reactive oxygen species levels at day 3,

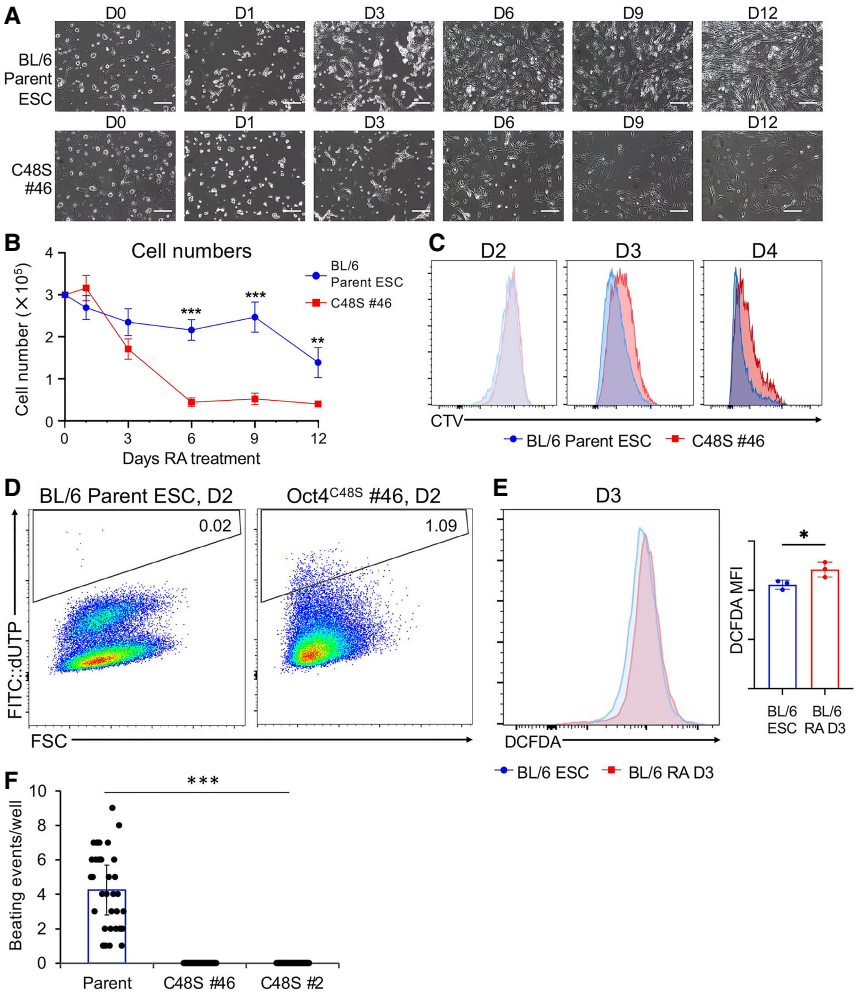

Figure 5. Oct4^{C48S} ESCs differentiate abnormally. (*A*) Phase-contrast images of parent and derived Oct4^{C48S} ESCs (clone #46) differentiated using RA for 12 days. Images were collected at the indicated times at 10× magnification. Scale bar, 0.2 mm. (*B*) Differentiating cells were trypsinized and counted using trypan blue exclusion using a hemacytometer. Cell counts ($N = 3$) were averaged and plotted. (*C*) Proliferation was measured in parent and C48S ESCs differentiating with RA at days 2–4. Cells were loaded with cell trace violet (CTV) at day 2. (*D*) TUNEL assay showing Oct4^{C48S} ESCs differentiated using RA. Cells were differentiated for 2 days and incubated with FITC-labeled dUTP for 1 h at 37°C prior to flow cytometry. (*E*) Undifferentiated and 3 day differentiating parent ESCs were incubated with DCFDA to assess ROS levels. (*F*) Parent and derived Oct4^{C48S} ESCs (clones #2 and #46) were differentiated into EBs, mesoderm lineage cells, and cardiomyocytes to assess beating. Average number of beating events per well is shown for $N = 36$ wells, with 10 EBs plated per well.

though specific oxidizing molecules at specific subcellular locations may be higher (Fig. 5E). Finally, we used mutant ESCs to form embryoid bodies (EBs) and subsequently generate cardiomyocytes. Differentiated cardiomyocytes form gap junctions, with functionality scorable by spontaneous and synchronous beating of groups of cells (Lynch et al. 2018). We found that unlike parent cells, which formed beating cardiomyocytes robustly, two different mutant ESC lines completely failed to form beating cells when differentiated (Fig. 5F; Supplemental Movies S1–S6). Beating was not rescued by extended culture, indicating that the phenotype was not kinetic in nature (data not shown). These results define a functional role for Oct4 Cys48 in ESC differentiation.

Oct4^{C48S} ESCs form less differentiated teratomas and contribute poorly to embryonic development

We used mutant and control ESC lines to form teratomas in mice, which were monitored for 2 weeks before tumor excision. Tumors were fixed, H&E stained, and pathologically scored in a blinded fashion. Parent tumors contained areas of maturing structures such as squamous tissue, respiratory epithelium (cilia and/or goblet cells), maturing neural components, gastric foveolar epithelium, and fat. In contrast, tumors formed with Oct4^{C48S} ESCs injected into the contralateral flanks of the same mice were more homogeneous with few maturing components, instead harboring immature neuroepithelial elements, immature cartilage, embryonal carcinoma, and yolk sac tumor (Fig. 6A,B). Additional images are shown in Supplemental Figure S11. Similar results were obtained using a wild-type and mutant teratomas derived from a different ESC line (Fig. 6C). At later time points, larger mutant teratomas began to accumulate mature structures, and the differences largely normalized (Supplemental Fig. S12).

One hallmark of pluripotency is the ability to contribute to cells and tissues of the embryo (De Los Angeles et al. 2015). We conducted chimerism assays to assess the ability of Oct4^{C48S} ESCs to contribute to development. We used eight lines of mutant ESCs derived from three parent lines of different strain backgrounds to minimize background and clonal effects. Compared with the parent cells, which contributed to offspring at a rate of 10%–15% (Fig. 6C), none of the derived Oct4^{C48S} ESCs were able to contribute to adult mice (Fig. 6D). The results indicate that Oct4^{C48S} ESCs contribute poorly to embryonic development. These results identify a role for Oct4 redox sensitivity in differentiation and development.

Oct4^{C48S} homozygous mutant mice show developmental lethality after the blastocyst stage

We generated germline mutant mouse lines with the Oct4^{C48S} mutation (dubbed *Janky* mice) using CRISPR modification of the endogenous *Pou5f1* gene. A heterozygous male founder was generated, which transmitted the *Jky* allele normally, as did its male and female offspring (Fig. 6E). In contrast, heterozygote intercrosses were associated with decreased litter sizes and a significant deviation from 1:2:1 Mendelian ratios, with homozygous *Jky* offspring severely attenuated (Fig. 6E). One *Jky* homozygous male was born to these crosses, which was phenotypically indistinguishable from its littermates at weaning but was sterile with underdeveloped testes (Supplemental Fig. S13A). Microscopic examination revealed significant heterogeneity in the size and diameter of the seminiferous tubules (Supplemental Fig. S13B). Immunofluorescence using spermatogonia and spermatocyte markers showed that a minority of seminiferous tubules had normal physiology (Box 1 in Supplemental Fig. S13C), but many displayed abnormal localization of spermatocytes and germ cell loss. Interestingly, the DNA damage marker γ-H2AX, which is normally associated with meiotic sex chromosome inactivation in pachytene spermatocytes (Fernandez-Capetillo et al. 2003), was not detected in *Jky*/*Jky* LIN28A^{+} spermatogonia, suggesting that loss of Oct4 redox sensing may regulate germ cell development but not spermatogonia maintenance. The developmental lethality associated with most embryos occurred after embryonic day 4.5, as blastocysts collected at this time genotyped as *Jky*/*Jky* at normal ratios (Fig. 6E). Collectively, these results identify Oct4 Cys48 as redox-sensitive and uncover dual roles for this residue in reprogramming and development.

Discussion

Oct4 protein levels must be precisely controlled for efficient iPSC reprogramming (Ilia et al. 2023) and exit from pluripotency (Wang et al. 2012; Aksoy et al. 2013; DeVeale et al. 2013). Nevertheless, the mechanisms by which Oct4 is post-transcriptionally regulated are poorly defined. Here, we pinpoint Oct4 redox sensitivity as an important determinant of both reprogramming and differentiation. Pluripotent cells coexpress Oct4 and Oct1 (Shen et al. 2017). Despite having similar DBDs and recognizing the same 8 bp consensus octamer sequence (Tantin 2013), Oct1 and other Oct4 paralogs do not function in reprogramming (Takahashi and Yamanaka 2006). Structure/function studies comparing Oct4 with these paralogs have identified different Oct4 reprogramming determinants (Esch et al. 2013; Jin et al. 2016; Jerabek et al. 2017; Boija et al. 2018). We identified Cys48 of the Oct4 DBD as a critical reprogramming determinant that sensitizes the protein to oxidative inhibition and degradation. In Oct1, this residue is a serine. Both residues hydrogen bond with the DNA phosphate backbone.

Transcription factors with both positive and negative roles in reprogramming include Oct4 and Smad3 (Ruetz et al. 2017; An et al. 2019; Velychko et al. 2019). Recent studies show that removal of Oct4 from reprogramming cocktails is inefficient but results in superior iPSC clones with enhanced developmental potential (An et al. 2019; Velychko et al. 2019). The counterproductive activity of Oct4 is due to promotion of off-target, ectoderm-specific gene expression (Velychko et al. 2019). These findings suggest that transient downregulation of counterproductive Oct4 activities may be an important step for efficient

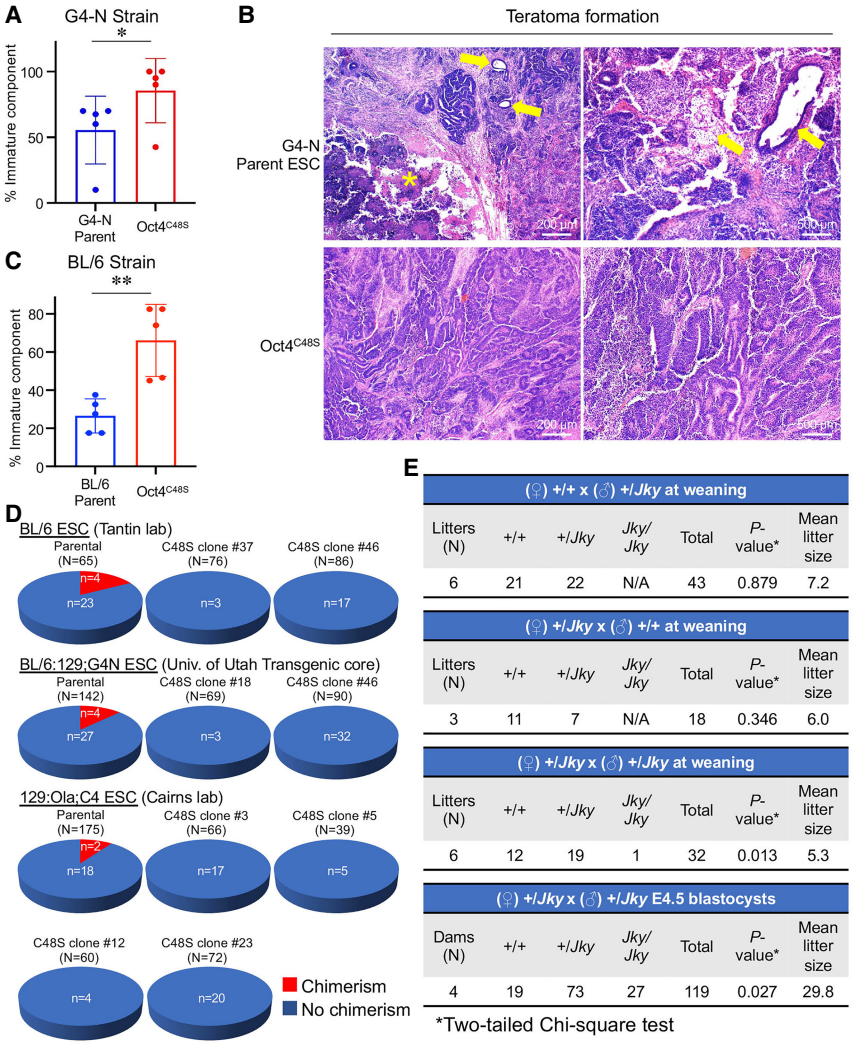

E

(♀) +/+ x (♂) +/*Jky* at weaning

Litters (N)	+/+	+/*Jky*	*Jky*/*Jky*	Total	*P*-value*	Mean litter size
6	21	22	N/A	43	0.879	7.2

(♀) +/*Jky* x (♂) +/+ at weaning

Litters (N)	+/+	+/*Jky*	*Jky*/*Jky*	Total	*P*-value*	Mean litter size
3	11	7	N/A	18	0.346	6.0

(♀) +/*Jky* x (♂) +/*Jky* at weaning

Litters (N)	+/+	+/*Jky*	*Jky*/*Jky*	Total	*P*-value*	Mean litter size
6	12	19	1	32	0.013	5.3

(♀) +/*Jky* x (♂) +/*Jky* E4.5 blastocysts

Dams (N)	+/+	+/*Jky*	*Jky*/*Jky*	Total	*P*-value*	Mean litter size
4	19	73	27	119	0.027	29.8

*Two-tailed Chi-square test

Figure 6. Oct4^{C48S} ESCs form teratomas lacking maturing structures and contribute poorly to adult chimeras. (*A*) We injected 1 × 10^6 parental or Oct4^{C48S} C57BL/6:129 ESCs (clone G4-N) into the contralateral flanks of NRG mice. After 15 days, tumors were harvested, fixed, sectioned, stained with H&E, deidentified, and scored pathologically. The percentage of cells within the tumor containing undifferentiated components was averaged and plotted. $N = 5$ independent tumors for each condition, combined from two separate experiments. For each tumor, values represent the average from a pair of slides. Two nonadjacent sections from each tumor were used. (*B*) Representative images are shown. Mature (differentiated) components (e.g., airway epithelium in teratomas derived from parental ESCs) are highlighted by yellow arrows. An asterisk indicates the area of necrosis. (*C*) Data similar to in *A*, except generated using an independently derived mutant from a different ESC line. $N = 5$ independent tumors. (*D*) Three different parent ESC lines and two to four derived lines of CRISPR-mutated Oct4^{C48S} ESCs were injected into recipient blastocysts ([*N*] number injected) and implanted into pseudopregnant animals. For each line, the proportion of chimeric offspring at weaning is shown as a pie chart. All karyotypes were confirmed to be similar to parent lines (between 72% and 92% normal). (*E*) Genotyping frequencies at weaning (postnatal day 24 [P24]) and embryonic day 4.5 (E4.5). Heterozygotes by wild-type crosses with different heterozygote genders are shown at the *top*. The *bottom* shows results from heterozygous intercrosses at P24 or E4.5. *P*-value was determined using a χ^2 test.

reprogramming. Our work suggests that Oct4 redox sensitivity fulfills such a role. The findings may provide a route to generating superior iPSC reprogramming outcomes with higher efficiency.

Oct4 is hypersensitive to oxidative stress (Lickteig et al. 1996; Guo et al. 2004; Marsboom et al. 2016) in a manner reversed by thioredoxin (Guo et al. 2004). Relative to other Oct proteins, Oct4 has unusually high cysteine content in the DBD, with two cysteines in each subdomain. Cys142 (Cys50 of the POU$_H$) lies in the recognition helix of POU$_H$ and is the distinguishing feature of POU$_H$s (Tantin 2013). Cys48 is located within the DNA recognition helix of the other DNA binding subdomain, POU$_S$. The hydrogen bond contact between Cys48 and the DNA predicts that cysteine oxidation will block DNA binding. Consistently, Oct4^{C48S} mutation maintains DNA binding and confers resistance to oxidation-induced DNA binding inhibition in vitro. The same mutation reduces reprogramming efficiency by more than half. Cysteine redox sensitivity is known to be enhanced by adjacent basic amino acid residues (Britto et al. 2002), and Cys48 is followed by a conserved Arg. Oct1 S48C mutation is sufficient to confer reprogramming activity but only in the context of the Oct4 N terminus. The Oct4 N terminus is known to mediate liquid–liquid phase transitions to control target gene transcription (Boija et al. 2018).

Prior studies have identified a link between Oct4 oxidation and degradation (Marsboom et al. 2016). Cys48 strongly promotes protein ubiquitylation, in particular following exposure to oxidative stress or MG-132. Oct4 is known to be polyubiquitylated by K63-linked chains via the action of the Stub1 E3 Ub ligase (Mamun et al. 2022); however, we found that K48-specific linkages were more strongly affected with Oct4^{C48S} mutation, suggesting a distinct pathway.

Endogenous Oct4^{C48S} mutation only minimally affects undifferentiated ESCs but results in abnormalities upon RA-mediated differentiation, including retention of Oct4 expression, deregulated gene expression, decreased proliferation, and increased apoptosis. Prominent roles for Oct4 in cell survival and proliferation during postimplantation embryonic development have been documented (DeVeale et al. 2013). When injected into adult mice, ESCs form teratomas containing differentiating structures representing

all three germ layers. When injected into blastocysts, they contribute to adult mouse tissues (De Los Angeles et al. 2015). We found that both features become defective with Cys48 mutation. Despite being gain of function, mice with this germline mutation (dubbed *Janky* mice) have no observed defects in the heterozygous condition. This may be due to a necessity for increased Oct4 activity above a certain threshold to trigger a phenotype. Homozygous *Jky* mutant mice undergo developmental lethality between E4.5 and birth. Given the timing of Oct4 expression during development, we predict that defects arise in these embryos at the blastocyst and/or peri-implantation stages, though this still awaits testing. Rare *Jky* mice obtained from these crosses appear normal at weaning, suggesting that mice circumventing this developmental restriction subsequently develop normally. However, the single male mouse that we obtained from these crosses was sterile. These findings are compatible with known roles for Oct4 in the germline (Schöler et al. 1990a; Kehler et al. 2004). The abnormal seminiferous tubule architecture of this mouse resembled the Pou5f1 TNAP-Cre conditional knockout (Kehler et al. 2004), suggesting a potentially central role for Oct4 redox regulation in the survival and migration of primordial germ cells. These results indicate that Cys48 is as important for differentiation and exit of pluripotency as it is for reprogramming and indicate a physiological role for Oct4 redox regulation through Cys48 during development.

Materials and methods

Cell culture

ESCs/iPSCs were cultured in Dulbecco's modified Eagle medium (Sigma) with "2iV" supplementation as described previously (Shakya et al. 2015; Shen et al. 2018). Media contained 15% fetal calf serum (FCS; Avantor), 2 mM L-glutamine (Thermo Fisher), 50 μM β-mercaptoethanol (2ME; Sigma), 1000 U/mL leukemia inhibitor factor (LIF; Chemicon), 0.1 mM minimal essential medium nonessential amino acids (NEAA; Thermo Fisher), 1 mM sodium pyruvate (Thermo Fisher), 1 μM MEK inhibitor PD03259010 (LC laboratories), and 3 μM glycogen synthase kinase-3β (GSK3β) inhibitor CHIR99021 (LC Laboratories). Culture medium was also supplemented with 50 μg/mL ascorbic acid (Sigma). H_2O_2 (Sigma) was supplied at 1 mM for 2 h, and MG-132 (Sigma) was supplied at 10 μM for 2 h. RA differentiation media omitted LIF, MEK inhibitor, and GSK3β inhibitor and contained retinoic acid (Sigma) at 1.5 μg/mL. Cardiomyocytes were generated using established protocols in which EBs were first generated via hanging drops and transferred to 12 well plates with differentiation medium (DMEM, 15% FCS, 2 mM L-glutamine, 0.1 mM NEAA, 1 mM sodium pyruvate, 0.1 mM 2ME, 50 μg/mL ascorbic acid) (Lynch et al. 2018). After 8 days in differentiation culture, cells were observed using an Olympus IX-51 inverted phase-contrast microscope. CTV proliferation assays were conducted using a kit (CTV proliferation kit for flow cytometry, Thermo Fisher). TUNEL assays were conducted using a kit (Apo-Direct, Becton-Dickinson). Alkaline phosphatase staining was performed using a kit (System Biosciences) according to the manufacturer's instructions. DCFDA staining was performed using a kit (AbCam) following the manufacturer's protocol.

FLAG-tagged lentiviral constructs for iPSC generation

The mSTEMCCA lentiviral vector expressing Oct4, Klf4, Sox2, and c-Myc was used for these studies (Somers et al. 2010). The Oct4 cDNA cassette was replaced with C-terminally FLAG-tagged full-length mouse Oct4, mouse Oct1, or chimeric constructs. FLAG-tagged Oct4 was generated by overlap PCR using primers containing the DYKDDDDK FLAG peptide sequence (Fwd: 5′-GATTA CAAGGATGACGACGATAAGGGAAGTGGCGTGAA ACAGA-3′; Rev: 5′-CTTATCGTCGTCATCCTTGTA ATCGTTTGAATGCATGGGAGAG-3′). The first fragment was amplified using a Fwd primer containing a NotI restriction enzyme site (5′-AATGAAAAAAGC GGCCGCCATGGCTGGACACCT-3′) and overlapping Rev primer containing the FLAG sequence. A second fragment was amplified using the Rev primer containing an NdeI restriction site (5′-GGGAATTCCATATGTGTGGC CATATTATCATCGTGT-3′) and overlapping Fwd primer. The first and second fragments were mixed as template and amplified Fwd and Rev primers containing NotI and NdeI. After purification and digestion with NotI and NdeI, the fragment was ligated with the mSTEMCCA vector digested by NotI and NdeI. Similar strategies were applied to generate other constructs. For point mutation, a site-directed mutagenesis kit (New England Biolabs Q5) was used. When making fusions between the different linker domains and POU_H, we maintained the "RKRKR" sequence at the N terminus of Oct4 POU_H, which has been shown to be important for reprogramming (Jerabek et al. 2017).

iPSC generation

293T cells were transfected with mSTEMCCA encoding FLAG-tagged Oct4, Oct1, and different domain swaps and mutants, as well as the packaging plasmids (pMDLg/pRRE and pRSV-Rev) and envelope plasmid (VSV-G), using polyethylenimine. Lentiviral supernatants were filtered, 8 μg/mL polybrene (Sigma) was added, and the mixture was used to transduce passage 3 primary MEFs expressing EGFP from the endogenous *Pou5f1* locus. The MEFs were prepared from E12.5 mouse embryos (Jackson Laboratories strain 008214, B6;129S4-Pou5f1^{tm2Jae}/J) and seeded in 6 well plates the night before transduction at a density of 1×10^5 cells/well. Cells were cultured in ESC medium (see above). GFP^+ iPSC colony emergence was quantified after 12 days using an Olympus IX-71 epifluorescence microscope. Lentivirus titers were established using two techniques. For the experiment shown in Supplemental Figure S2B, a kit measuring p24 was used (QuickTiter lentivirus titer kit, Cell Biolabs). For the experiment shown in Supplemental Figure S4C,

a kit measuring conserved areas of viral RNA was used (Lenti-X qRT-PCR, Takara Bio).

Immunoblotting and immunofluorescence

Antibodies used for immunoblotting were Oct4, α-tubulin, and β-actin from Santa Cruz Biotechnology; Oct1 from Bethyl Laboratories; Nanog and Sox2 from GeneTex; GAPDH from EMD Millipore; FK2 (pan-Ub) from Enzo Life Sciences; and Ub-K48 from Cell Signaling Technology. All immunoblots are shown in uncropped form in Supplemental Figures S14–S17. For immunofluorescence, testes from both an *Oct4*$^{Jky/Jky}$ mouse and an *Oct4*$^{+/+}$ littermate control were weighed and fixed using 4% formaldehyde. The paraffinized testes were sectioned into 5 µm slices. Antibodies used for immunofluorescence were mouse anti-SYCP3 from Santa Cruz Biotechnology; goat anti-LIN28A from R&D Systems; rabbit anti-phospho-H2AX from Cell Signaling Technology; and Alex fluor 647 donkey antimouse IgG, Alex fluor 488 donkey anti-rabbit IgG, and Alex fluor 594 donkey antigoat IgG from Thermo Fisher Scientific. Data were imaged using a Nikon Eclipse Ti inverted microscope with Nikon Elements AR software.

Electrophoretic mobility shift assay

EMSA was performed using published methods (Kang et al. 2009; Ferraris et al. 2011). Diamide (Sigma) was added at a final concentration of up to 300 µM on ice during reaction assembly. The 5′Cy5-labeled double-stranded DNA probes used were as follows: wild-type octamer (5′-TGTCGAATGCAAATCACT-3′) and mutant octamer (5′-TGTCGAATGCAAGCCACT-3′). Reactions were incubated for 30 min at room temperature prior to gel loading. For experiments involving reversal of oxidative inhibition, thioredoxin (Sigma) was supplied at a final concentration of 0–60 µM after 15 min of incubation with diamide, and both thioredoxin-treated and control samples were incubated for a further 15 min at 37°C prior to gel loading. DNA was visualized using a Molecular Dynamics Typhoon system.

Recombinant Oct4 protein

Wild-type and C48S Oct4 constructs were generated bearing dual C-terminal FLAG and twin-strep tags. A g-block (IDT) fragment coding for the twin-strep and FLAG epitope tags was inserted between the NcoI and KpnI sites in the transient expression vector pACE-MAM2 (Geneva Biotech). The resultant construct was then digested with NcoI and PvuII to insert the g-block fragment coding for either wild-type or C48S murine Oct4. After Sanger sequencing to confirm veracity, the plasmids were transfected into Expi293F cells (Thermo Fisher) using the ExpiFectamine 293 transfection kit (Thermo Fisher) following the manufacturer's instructions. After 2 days, transfected cells were harvested and washed with ice-cold PBS. Cells were resuspended in buffer A (20 mM HEPES at pH 8.0, 1.5 mM $MgCl_2$, 10 mM KCl, 0.25% NP-40, 0.5 mM DTT, 2× protease inhibitor cocktail [Roche]), incubated for 10 min on ice, and homogenized using a Dounce homogenizer (Wheaton). The homogenate was centrifuged at 3800*g* for 5 min at 4°C. Pelleted nuclei were resuspended in buffer C (20 mM HEPES at pH 8.0, 25% glycerol, 1.5 mM $MgCl_2$, 420 mM KCl, 0.25% NP-40, 0.2 mM EDTA, 0.5 mM DTT, 2× protease inhibitor cocktail) and Dounce homogenized again. Nuclei were extracted for 30 min at 4°C with end-to-end rotation and then centrifuged at 20,000*g* for 30 min at 4°C. The nuclear extract was then subjected to immunoprecipitation with anti-FLAG (M2)-agarose beads (Sigma). Bead-bound proteins were eluted with 200 ng/µL 3xFLAG peptide (Sigma) by incubation for 30 min at 4°C. The protein was pure and monodisperse, as verified using Coomassie blue staining and size exclusion chromatography.

Generation of Oct4^{C48S} *mouse ESCs*

Mutant ESCs with a single-base missense mutation that converts Cys48 to Ser were generated using templated CRISPR. A modified synthetic sgRNA (Synthego) was designed to target Cas9 and cut near the target nucleotide (5′-GGCCTCGAAGCGACAGATGG-3′, where the underlined C indicates the target nucleotide). The sgRNA was complexed with Cas9 protein (IDT) to form a ribonucleoprotein (RNP) complex that was electroporated with program CG-104 into 6×10^4 mouse ESCs using a LONZA 4D-nucleofector X unit. The RNP was coelectroporated with a corresponding single-stranded oligodeoxynucleotide (ssODN) with 5′ and 3′ phosphorothioate modifications (5′-ctcactctgtttgatcggcctttcagGAAAGGTGTTCAG CCAGACCA**CCATCTCTAGATTCGAGGCC**TTGCAG CTCAGCCTTAAGAACATGTGTAAGCTG-3′, where lowercase denotes intronic sequence, and the sgRNA site is in bold). The ssODN contained the target mutation (underlined) and silent mutations in the seed region (double underlined) to block CRISPR recutting after incorporation of the donor and to generate a unique XbaI restriction enzyme site for screening purposes. Incorporation of the ssODN sequence was identified via PCR and restriction enzyme digestion and confirmed by sequencing of the 709 bp region flanking the mutation. Mutant clones were generated from a pure C57BL/6 ESC line, a 129/BL6 hybrid line expressing constitutive GFP, and a reporter line used to dedifferentiate ESCs into a 2C-like state. Clones were tested by karyotype, and any clones with <70% normal diploid content were excluded.

RNA-seq

ESCs were first depleted by feeder cells by incubation on plates coated with gelatin. Parental and derived Oct4^{C48S} ESC lines were differentiated in media lacking LIF and containing 1.5 mg/L RA for 2 days. Undifferentiated and RA-differentiated cells were collected, and RNA was prepared using a kit (RNeasy; Qiagen). RNA poly(A) was selected for mRNA using NEBNext rRNA depletion kit v2 (humans, mice, and rats) (E7400). Bulk RNA was processed and sequenced as reported previously (Perovanovic

et al. 2023). Briefly, RNA-seq reads were aligned to GRCh38/hg38 using STAR version 2.7.9a. Read counts were normalized using the DESeq2 analysis package. The DESeq2-regularized log transformation was applied to counts, which preferentially shrank the overall variance among low-abundance transcripts. The high-throughput data are available on the Gene Expression Omnibus (GEO) server under series record GSE241332. Differential genes were identified using 2.5-fold change and $P < 0.001$ as cutoffs. GO terms were identified using PANTHER (Mi et al. 2013).

Teratoma formation

All animal experiments were approved by the University of Utah Institutional Animal Care and Use Committee. Feeder-depleted parental and derived Oct4^{C48S} ESC lines were injected subcutaneously into the contralateral flanks of 6–8 week old female NOD.*Rag1*$^{-/-}$*Il2rg*$^{-/-}$ (NRG; Jackson Laboratories) mice to generate teratomas; 1×10^6 cells were implanted. After 2 weeks, mice were humanely euthanized, and tumors were excised. After fixation, embedding, and sectioning, slides were stained with H&E and evaluated in a blinded fashion.

Chimeric mouse assays

Targeted or parental ESCs were collected and resuspended in injection medium consisting of DMEM with HEPES (Thermo Fisher) supplemented with 10% FBS (peak serum) and 0.1 mM 2-mercaptoethanol (Sigma). C57B6 clones were injected into albino B6 blastocysts, while the G4N and C4 clones (B6:129 and 129 in origin, respectively) were injected into C57B6 blastocysts. E3.5 blastocysts were used. Ten to 25 ESCs were injected into each blastocyst using micromanipulators (Eppendorf) and a Leica inverted microscope. After culturing injected blastocysts in KSOM (CytoSpring), ~12–18 blastocysts were surgically transferred into the uterine horns of day 2.5 pseudopregnant mice or the oviducts of day 0.5 pseudopregnant mice. Mice were scored based on coat and eye color by members of the Transgenic Core Facility at weaning.

Janky *mice*

Mutant C57BL6/J mice with a single-base missense mutation that converts Cys48 to Ser (*Jky* mice) were generated using the same templated CRISPR strategy used to generate mutant ESCs. CRISPR RNPs were introduced into single-cell C57BL6/J mouse embryos using pronuclear injection. Founder mice that carried the targeted mutation were backcrossed to WT, and the N1 generation was sequenced to confirm the presence of the heterozygous allele.

Statistical analyses

All pairwise data comparisons used two-tailed student *t*-tests except for Figure 6A, for which the *P*-value was generated using an unpaired one-tailed *t*-test. Data points were symmetrically distributed around means. Asterisks in the figures depict $P < 0.05$ (*), $P < 0.01$ (**), and $P < 0.001$ (***). All error bars depict ±standard deviation. The significance of deviation from Mendelian inheritance patterns was determined by χ^2 testing.

Data availability

All numerical raw data associated with the figures have been uploaded to the Dryad database (doi:10.5061/dryad.05qfttfbf).

Competing interest statement

The authors declare no competing interests.

Acknowledgments

We thank S. Buckley for critical reading of the manuscript. We thank C. Davey, H. Lan, and the University of Utah Mouse Transgenic and Gene Targeting Core, as well as the Mutation Generation and Detection Core, for assistance with CRISPR-edited ESC lines, chimerism assays, karyotyping, and the generation of germline mutant mice. We thank B. Dalley and the High-Throughput Genomics Core Facility, and Q. Li and the Bioinformatics Analysis Core Facility for assistance with RNA-seq. We thank D. Lum and the Preclinical Research Resource Core Facility for assistance with teratoma formation. We thank J. Marvin and the Flow Cytometry Core, and X. Wang and the Cell Imaging Core. We thank B. Weaver for the gift of the C4 ESC line. This work was supported by National Institutes of Health/National Institute of General Medical Sciences grant R01GM122778 to D.T.

Author contributions: D.T. conceived the study. Z.S., Y.W., and D.T. designed the experiments. Z.S., Y.W., and M.B.C. generated new reagents for the study. Z.S., Y.W., A.M., C.Y., B.R.C., and K.J.E. performed the experiments and/or analyzed the data. K.J.E. performed blinded pathological analysis of teratoma samples. Z.S., Y.W., and A.M. generated the figures. All authors contributed to the writing of the manuscript and read and approved the final version of the manuscript prior to submission for publication.

References

Aksoy I, Jauch R, Chen J, Dyla M, Divakar U, Bogu GK, Teo R, Leng Ng CK, Herath W, Lili S, et al. 2013. Oct4 switches partnering from Sox2 to Sox17 to reinterpret the enhancer code and specify endoderm. *EMBO J* **32:** 938–953. doi:10.1038/emboj.2013.31

An Z, Liu P, Zheng J, Si C, Li T, Chen Y, Ma T, Zhang MQ, Zhou Q, Ding S. 2019. Sox2 and Klf4 as the functional core in pluripotency induction without exogenous Oct4. *Cell Rep* **29:** 1986–2000.e8. doi:10.1016/j.celrep.2019.10.026

Boija A, Klein IA, Sabari BR, Dall'Agnese A, Coffey EL, Zamudio AV, Li CH, Shrinivas K, Manteiga JC, Hannett NM, et al. 2018. Transcription factors activate genes through the phase-separation capacity of their activation domains. *Cell* **175:** 1842–1855.e16. doi:10.1016/j.cell.2018.10.042

Boyer LA, Lee TI, Cole MF, Johnstone SE, Levine SS, Zucker JP, Guenther MG, Kumar RM, Murray HL, Jenner RG, et al. 2005. Core transcriptional regulatory circuitry in human embryonic stem cells. *Cell* **122:** 947–956. doi:10.1016/j.cell.2005.08.020

Britto PJ, Knipling L, Wolff J. 2002. The local electrostatic environment determines cysteine reactivity of tubulin. *J Biol Chem* **277:** 29018–29027. doi:10.1074/jbc.M204263200

Buganim Y, Markoulaki S, van Wietmarschen N, Hoke H, Wu T, Ganz K, Akhtar-Zaidi B, He Y, Abraham BJ, Porubsky D, et al. 2014. The developmental potential of iPSCs is greatly influenced by reprogramming factor selection. *Cell Stem Cell* **15:** 295–309. doi:10.1016/j.stem.2014.07.003

Chen J, Gao Y, Huang H, Xu K, Chen X, Jiang Y, Li H, Gao S, Tao Y, Wang H, et al. 2015. The combination of Tet1 with Oct4 generates high-quality mouse-induced pluripotent stem cells. *Stem Cells* **33:** 686–698. doi:10.1002/stem.1879

Costa Y, Ding J, Theunissen TW, Faiola F, Hore TA, Shliaha PV, Fidalgo M, Saunders A, Lawrence M, Dietmann S, et al. 2013. NANOG-dependent function of TET1 and TET2 in establishment of pluripotency. *Nature* **495:** 370–374. doi:10.1038/nature11925

De Los Angeles A, Ferrari F, Xi R, Fujiwara Y, Benvenisty N, Deng H, Hochedlinger K, Jaenisch R, Lee S, Leitch HG, et al. 2015. Hallmarks of pluripotency. *Nature* **525:** 469–478. doi:10.1038/nature15515

DeVeale B, Brokhman I, Mohseni P, Babak T, Yoon C, Lin A, Onishi K, Tomilin A, Pevny L, Zandstra PW, et al. 2013. Oct4 is required ~E7.5 for proliferation in the primitive streak. *PLoS Genet* **9:** e1003957. doi:10.1371/journal.pgen.1003957

Esch D, Vahokoski J, Groves MR, Pogenberg V, Cojocaru V, Vom Bruch H, Han D, Drexler HC, Araúzo-Bravo MJ, Ng CK, et al. 2013. A unique Oct4 interface is crucial for reprogramming to pluripotency. *Nat Cell Biol* **15:** 295–301. doi:10.1038/ncb2680

Esteban MA, Wang T, Qin B, Yang J, Qin D, Cai J, Li W, Weng Z, Chen J, Ni S, et al. 2010. Vitamin C enhances the generation of mouse and human induced pluripotent stem cells. *Cell Stem Cell* **6:** 71–79. doi:10.1016/j.stem.2009.12.001

Evans MJ, Kaufman MH. 1981. Establishment in culture of pluripotential cells from mouse embryos. *Nature* **292:** 154–156. doi:10.1038/292154a0

Feng B, Jiang J, Kraus P, Ng JH, Heng JC, Chan YS, Yaw LP, Zhang W, Loh YH, Han J, et al. 2009. Reprogramming of fibroblasts into induced pluripotent stem cells with orphan nuclear receptor Esrrb. *Nat Cell Biol* **11:** 197–203. doi:10.1038/ncb1827

Fernandez-Capetillo O, Mahadevaiah SK, Celeste A, Romanienko PJ, Camerini-Otero RD, Bonner WM, Manova K, Burgoyne P, Nussenzweig A. 2003. H2AX is required for chromatin remodeling and inactivation of sex chromosomes in male mouse meiosis. *Dev Cell* **4:** 497–508. doi:10.1016/S1534-5807(03)00093-5

Ferraris L, Stewart AP, Kang J, DeSimone AM, Gemberling M, Tantin D, Fairbrother WG. 2011. Combinatorial binding of transcription factors in the pluripotency control regions of the genome. *Genome Res* **21:** 1055–1064. doi:10.1101/gr.115824.110

Gao Y, Chen J, Li K, Wu T, Huang B, Liu W, Kou X, Zhang Y, Huang H, Jiang Y, et al. 2013. Replacement of Oct4 by Tet1 during iPSC induction reveals an important role of DNA methylation and hydroxymethylation in reprogramming. *Cell Stem Cell* **12:** 453–469. doi:10.1016/j.stem.2013.02.005

Guo Y, Einhorn L, Kelley M, Hirota K, Yodoi J, Reinbold R, Scholer H, Ramsey H, Hromas R. 2004. Redox regulation of the embryonic stem cell transcription factor Oct-4 by thioredoxin. *Stem Cells* **22:** 259–264. doi:10.1634/stemcells.22-3-259

Han D, Wu G, Chen R, Drexler HCA, MacCarthy CM, Kim KP, Adachi K, Gerovska D, Mavrommatis L, Bedzhov I, et al. 2022. A balanced Oct4 interactome is crucial for maintaining pluripotency. *Sci Adv* **8:** eabe4375. doi:10.1126/sciadv.abe4375

Heng JC, Feng B, Han J, Jiang J, Kraus P, Ng JH, Orlov YL, Huss M, Yang L, Lufkin T, et al. 2010. The nuclear receptor Nr5a2 can replace Oct4 in the reprogramming of murine somatic cells to pluripotent cells. *Cell Stem Cell* **6:** 167–174. doi:10.1016/j.stem.2009.12.009

Ilia K, Shakiba N, Bingham T, Jones RD, Kaminski MM, Aravera E, Bruno S, Palacios S, Weiss R, Collins JJ, et al. 2023. Synthetic genetic circuits to uncover the OCT4 trajectories of successful reprogramming of human fibroblasts. *Sci Adv* **9:** eadg8495. doi:10.1126/sciadv.adg8495

Jerabek S, Ng CK, Wu G, Arauzo-Bravo MJ, Kim KP, Esch D, Malik V, Chen Y, Velychko S, MacCarthy CM, et al. 2017. Changing POU dimerization preferences converts Oct6 into a pluripotency inducer. *EMBO Rep* **18:** 319–333. doi:10.15252/embr.201642958

Jin W, Wang L, Zhu F, Tan W, Lin W, Chen D, Sun Q, Xia Z. 2016. Critical POU domain residues confer Oct4 uniqueness in somatic cell reprogramming. *Sci Rep* **6:** 20818. doi:10.1038/srep20818

Kang J, Gemberling M, Nakamura M, Whitby FG, Handa H, Fairbrother WG, Tantin D. 2009. A general mechanism for transcription regulation by Oct1 and Oct4 in response to genotoxic and oxidative stress. *Genes Dev* **23:** 208–222. doi:10.1101/gad.1750709

Kehler J, Tolkunova E, Koschorz B, Pesce M, Gentile L, Boiani M, Lomeli H, Nagy A, McLaughlin KJ, Schöler HR, et al. 2004. Oct4 is required for primordial germ cell survival. *EMBO Rep* **5:** 1078–1083. doi:10.1038/sj.embor.7400279

Kim KP, Wu Y, Yoon J, Adachi K, Wu G, Velychko S, MacCarthy CM, Shin B, Röpke A, Arauzo-Bravo MJ, et al. 2020. Reprogramming competence of OCT factors is determined by transactivation domains. *Sci Adv* **6:** eaaz7364. doi:10.1126/sciadv.aaz7364

King HW, Klose RJ. 2017. The pioneer factor OCT4 requires the chromatin remodeller BRG1 to support gene regulatory element function in mouse embryonic stem cells. *Elife* **6:** e22631. doi:10.7554/eLife.22631

Klemm JD, Rould MA, Aurora R, Herr W, Pabo CO. 1994. Crystal structure of the Oct-1 POU domain bound to an octamer site: DNA recognition with tethered DNA-binding modules. *Cell* **77:** 21–32. doi:10.1016/0092-8674(94)90231-3

Lengner CJ, Camargo FD, Hochedlinger K, Welstead GG, Zaidi S, Gokhale S, Scholer HR, Tomilin A, Jaenisch R. 2007. Oct4 expression is not required for mouse somatic stem cell self-renewal. *Cell Stem Cell* **1:** 403–415. doi:10.1016/j.stem.2007.07.020

Lickteig K, Lamb K, Brigman K, Rizzino A. 1996. Effects of oxidation and reduction on the binding of transcription factors to *cis*-regulatory elements located in the FGF-4 gene. *Mol Reprod Dev* **44:** 146–152. doi:10.1002/(SICI)1098-2795(199606)44:2<146::AID-MRD2>3.0.CO;2-N

Lynch AT, Mazzotta S, Hoppler S. 2018. Cardiomyocyte differentiation from mouse embryonic stem cells. *Methods Mol Biol* **1816:** 55–66. doi:10.1007/978-1-4939-8597-5_4

Mamun MMA, Khan MR, Zhu Y, Zhang Y, Zhou S, Xu R, Bukhari I, Thorne RF, Li J, Zhang XD, et al. 2022. Stub1 maintains proteostasis of master transcription factors in embryonic stem cells. *Cell Rep* **39:** 110919. doi:10.1016/j.celrep.2022.110919

Marsboom G, Zhang GF, Pohl-Avila N, Zhang Y, Yuan Y, Kang H, Hao B, Brunengraber H, Malik AB, Rehman J. 2016. Glutamine metabolism regulates the pluripotency transcription factor Oct4. *Cell Rep* **16:** 323–332. doi:10.1016/j.celrep.2016.05.089

Mi H, Muruganujan A, Casagrande JT, Thomas PD. 2013. Large-scale gene function analysis with the PANTHER classification system. *Nat Protoc* **8:** 1551–1566. doi:10.1038/nprot.2013.092

Michael AK, Grand RS, Isbel L, Cavadini S, Kozicka Z, Kempf G, Bunker RD, Schenk AD, Graff-Meyer A, Pathare GR, et al. 2020. Mechanisms of OCT4–SOX2 motif readout on nucleosomes. *Science* **368:** 1460–1465. doi:10.1126/science.abb0074

Morey L, Santanach A, Di Croce L. 2015. Pluripotency and epigenetic factors in mouse embryonic stem cell fate regulation. *Mol Cell Biol* **35:** 2716–2728. doi:10.1128/MCB.00266-15

Nakagawa M, Koyanagi M, Tanabe K, Takahashi K, Ichisaka T, Aoi T, Okita K, Mochiduki Y, Takizawa N, Yamanaka S. 2008. Generation of induced pluripotent stem cells without Myc from mouse and human fibroblasts. *Nat Biotechnol* **26:** 101–106. doi:10.1038/nbt1374

Nichols J, Zevnik B, Anastassiadis K, Niwa H, Klewe-Nebenius D, Chambers I, Schöler H, Smith A. 1998. Formation of pluripotent stem cells in the mammalian embryo depends on the POU transcription factor Oct4. *Cell* **95:** 379–391. doi:10.1016/S0092-8674(00)81769-9

Okamoto K, Okazawa H, Okuda A, Sakai M, Muramatsu M, Hamada H. 1990. A novel octamer binding transcription factor is differentially expressed in mouse embryonic cells. *Cell* **60:** 461–472. doi:10.1016/0092-8674(90)90597-8

Perovanovic J, Wu Y, Abewe H, Shen Z, Hughes EP, Gertz J, Chandrasekharan MB, Tantin D. 2023. Oct1 cooperates with the smad family of transcription factors to promote mesodermal lineage specification. *Sci Signal* **16:** eadd5750. doi:10.1126/scisignal.add5750

Radzisheuskaya A, Le Bin Chia G, Dos Santos RL, Theunissen TW, Castro LF, Nichols J, Silva JC. 2013. A defined Oct4 level governs cell state transitions of pluripotency entry and differentiation into all embryonic lineages. *Nat Cell Biol* **15:** 579–590. doi:10.1038/ncb2742

Rais Y, Zviran A, Geula S, Gafni O, Chomsky E, Viukov S, Mansour AA, Caspi I, Krupalnik V, Zerbib M, et al. 2013. Deterministic direct reprogramming of somatic cells to pluripotency. *Nature* **502:** 65–70. doi:10.1038/nature12587

Rosner MH, Vigano MA, Ozato K, Timmons PM, Poirier F, Rigby PW, Staudt LM. 1990. A POU-domain transcription factor in early stem cells and germ cells of the mammalian embryo. *Nature* **345:** 686–692. doi:10.1038/345686a0

Ruetz T, Pfisterer U, Di Stefano B, Ashmore J, Beniazza M, Tian TV, Kaemena DF, Tosti L, Tan W, Manning JR, et al. 2017. Constitutively active SMAD2/3 are broad-scope potentiators of transcription-factor-mediated cellular reprogramming. *Cell Stem Cell* **21:** 791–805.e9. doi:10.1016/j.stem.2017.10.013

Schöler HR, Dressler GR, Balling R, Rohdewohld H, Gruss P. 1990a. Oct-4: a germline-specific transcription factor mapping to the mouse t-complex. *EMBO J* **9:** 2185–2195. doi:10.1002/j.1460-2075.1990.tb07388.x

Schöler HR, Ruppert S, Suzuki N, Chowdhury K, Gruss P. 1990b. New type of POU domain in germ line-specific protein Oct-4. *Nature* **344:** 435–439. doi:10.1038/344435a0

Shakya A, Callister C, Goren A, Yosef N, Garg N, Khoddami V, Nix D, Regev A, Tantin D. 2015. Pluripotency transcription factor Oct4 mediates stepwise nucleosome demethylation and depletion. *Mol Cell Biol* **35:** 1014–1025. doi:10.1128/MCB.01105-14

Shen Z, Kang J, Shakya A, Tabaka M, Jarboe EA, Regev A, Tantin D. 2017. Enforcement of developmental lineage specificity by transcription factor Oct1. *Elife* **6:** e20937. doi:10.7554/eLife.20937

Shen Z, Formosa T, Tantin D. 2018. FACT inhibition blocks induction but not maintenance of pluripotency. *Stem Cells Dev* **27:** 1693–1701. doi:10.1089/scd.2018.0150

Shi Y, Desponts C, Do JT, Hahm HS, Schöler HR, Ding S. 2008. Induction of pluripotent stem cells from mouse embryonic fibroblasts by Oct4 and Klf4 with small-molecule compounds. *Cell Stem Cell* **3:** 568–574. doi:10.1016/j.stem.2008.10.004

Somers A, Jean JC, Sommer CA, Omari A, Ford CC, Mills JA, Ying L, Sommer AG, Jean JM, Smith BW, et al. 2010. Generation of transgene-free lung disease-specific human induced pluripotent stem cells using a single excisable lentiviral stem cell cassette. *Stem Cells* **28:** 1728–1740. doi:10.1002/stem.495

Sommer CA, Stadtfeld M, Murphy GJ, Hochedlinger K, Kotton DN, Mostoslavsky G. 2009. Induced pluripotent stem cell generation using a single lentiviral stem cell cassette. *Stem Cells* **27:** 543–549. doi:10.1634/stemcells.2008-1075

Soufi A, Donahue G, Zaret KS. 2012. Facilitators and impediments of the pluripotency reprogramming factors' initial engagement with the genome. *Cell* **151:** 994–1004. doi:10.1016/j.cell.2012.09.045

Suzuki N, Rohdewohld H, Neuman T, Gruss P, Schöler HR. 1990. Oct-6: a POU transcription factor expressed in embryonal stem cells and in the developing brain. *EMBO J* **9:** 3723–3732. doi:10.1002/j.1460-2075.1990.tb07585.x

Takahashi K, Yamanaka S. 2006. Induction of pluripotent stem cells from mouse embryonic and adult fibroblast cultures by defined factors. *Cell* **126:** 663–676. doi:10.1016/j.cell.2006.07.024

Tantin D. 2013. Oct transcription factors in development and stem cells: insights and mechanisms. *Development* **140:** 2857–2866. doi:10.1242/dev.095927

Velychko S, Adachi K, Kim KP, Hou Y, MacCarthy CM, Wu G, Schöler HR. 2019. Excluding Oct4 from Yamanaka cocktail unleashes the developmental potential of iPSCs. *Cell Stem Cell* **25:** 737–753.e4. doi:10.1016/j.stem.2019.10.002

Vierbuchen T, Wernig M. 2012. Molecular roadblocks for cellular reprogramming. *Mol Cell* **47:** 827–838. doi:10.1016/j.molcel.2012.09.008

Wang Z, Oron E, Nelson B, Razis S, Ivanova N. 2012. Distinct lineage specification roles for NANOG, OCT4, and SOX2 in human embryonic stem cells. *Cell Stem Cell* **10:** 440–454. doi:10.1016/j.stem.2012.02.016

Yuan X, Wan H, Zhao X, Zhu S, Zhou Q, Ding S. 2011. Combined chemical treatment enables *Oct4*-induced reprogramming from mouse embryonic fibroblasts. *Stem Cells* **29:** 549–553. doi:10.1002/stem.594